International Journal of Thermal Sciences 49 (2010) 1086–1094

Contents lists available at ScienceDirect

International Journal of Thermal Sciences

journal homepage: www.elsevier.com/locate/ijts

Heat transfer characteristics of flow boiling in a single horizontal microchannel

Gian Piero Celata [a,*], Sujoy Kumar Saha [b], Giuseppe Zummo [a], Denam Dossevi [a]

[a] ENEA Casaccia Research Centre, Institute of Thermal Fluid Dynamics, Office Building F-20, Via Anguillarese 301, 00123 S. M. Galeria, Roma, Italy
[b] Mechanical Engineering Department, Bengal Engineering and Science University, Shibpur, Howrah 711 103, West Bengal, India

ARTICLE INFO

Article history:
Received 16 October 2009
Received in revised form
18 January 2010
Accepted 20 January 2010
Available online 19 February 2010

Keywords:
Heat transfer
Subcooled flow boiling
Microchannel
Instability
Flow pattern

ABSTRACT

Heat transfer characteristics of subcooled flow boiling of FC-72 in a single horizontal circular cross-section microchannel (480 μm i.d., 800 μm o.d., 102 mm long) are presented. Different flow patterns, both in the stable and unstable flow boiling regimes, have been captured using high speed video camera. Data in small, medium, high and very high heat flux cases under small, medium and high mass flux has been presented. Convective heat transfer coefficients in each flow boiling situation have been calculated and presented. Stable flow boiling with alternating bubbly/slug flow, slug/annular flow and annular/mist flow have been observed for heat flux of 150 kW/m^2 or higher and mass flux of 1500 kg/m^2 s or higher. Back and forth oscillations with flow instabilities have been observed in cases of lower heat and mass fluxes. However, no complete reverse flow in upstream direction has been observed.

1. Introduction

Microsystems are widely used in high heat flux situations due to their low cost and high potential applications in many fields such as space, communication, biology and industry. Microchannels are used in MEMS and high-end microprocessors cooling applications. Phase-change processes like flow boiling are very important in such devices. The understanding of thermal and flow behaviour on a microscale is very important. Bubble dynamics in microchannel is quite different from that in an ordinary sized channel. Bubble growth in a microchannel is restrained by the channel wall and in the transverse direction. The two-phase flow pattern, observed simultaneously in the channels may be different, depending on heat and mass fluxes.

Boiling is desirable in microchannel heat sinks for more probable uniform wall temperature since then wall temperature is constrained to the fluid saturation temperature. The flow rate in microchannels is low to contain the pressure drop. Therefore, large enthalpy rise of the fluid for high heat flux is inevitable. Small microchannel flow boiling systems are sensitive to oscillatory instabilities.

Different aspects of flow boiling in small channels are found in [1–13]. Wang et al. [14] have studied experimentally the stable and unstable flow boiling in parallel microchannels and in a single microchannel.

Among the various aspects encountered in small channels, two-phase flow heat transfer, flow pattern and pressure drop have been extensively investigated in last decade, [1,2,15–23].

In this paper, heat transfer characteristics of subcooled flow boiling of FC-72 in a single horizontal microchannel are presented. Experimental set up and operating procedure is described in Section 2. Data reduction method is discussed in Section 3. Results of the present experiments are presented and discussed in Section 4. Conclusions are drawn in Section 5.

2. Experimental set up and operating procedure

The experimental facility as shown in Fig. 1 consists of:

- A tank of helium for the pressurization and release of FC-72 from the tank
- A tank for the storage of the FC-72
- An inlet valve for the control of pressure and mass flow rate in the test section
- A preheater for the control of the subcooled temperature of FC-72
- A venting point to avoid bubble at the inlet of the test section
- The test section
- A scale

* Corresponding author.
E-mail addresses: celata@enea.it (G.P. Celata), sujoy_k_saha@hotmail.com (S.K. Saha), zummo@enea.it (G. Zummo), dossevidenam@aol.com (D. Dossevi).

1290-0729/$ – see front matter © 2010 Elsevier Masson SAS. All rights reserved.
doi:10.1016/j.ijthermalsci.2010.01.019

Nomenclature

Cp	specific heat (J kg^{-1} K^{-1})
D	diameter (m)
G	mass flux (kg/m^{-2} s^{-1})
L	length (m)
h	heat transfer coefficient (W m^{-2} K^{-1})
H_{lv}	latent heat of vaporization (J kg^{-1})
$\dot{m}$	mass flow rate (kg s^{-1})
P	pressure (bar)
Pr	Prandtl number
Q	heat (W)
q	heat flux (kW/m^2)
R	thermal resistance (K W^{-1})
Re	Reynolds number
S	area (m^2)
T	temperature (K)
V	velocity (m s^{-1})
x	vapour quality

Subscripts

ext	external
cs	cross-sectional
in	inlet
int	internal
l	liquid
loss	loss
out	outlet
sat	saturation
sp	single phase
tp	two phase
v	vapour
w	wall
wat	water

Greeks

μ	dynamic viscosity
λ	thermal conductivity
ρ	density

The preheater consists of two elements. The first element is a water heater and the second is a coiled tube. FC-72 flows in the tube. The coiled tube is dipped in the water heater and by changing the water temperature; the FC-72 inlet temperature is controlled. Just after this system, there is a venting point to avoid bubble in the inlet of the test section. The test section is shown in Fig. 2. It consists of a pool of water or propylene glycol in which is dipped the perfectly aligned horizontal single microchannel. The pool is composed of a Teflon cylinder and two plates of polycarbonate. The microchannel is made of Pyrex. Table 1 gives the details of the components including the test section dimensions.

FC-72 is heated in the microchannel by indirect heating with water or propylene glycol and the water or glycol temperature in the pool is controlled by a water or glycol heater. At the inlet and at the outlet of the test section, there are thermocouples which give temperatures of the room, of the water or glycol and of FC-72. There is one sensor to measure the inlet pressure of the fluid. Finally there is a scale. After passing through the test section, the fluid (FC-72) is led to a scale which gives the value of the mass flow rate.

During the experiments, the system pressure, the mass flow rate, the sub-cooled temperature and the water or glycol temperature are controlled. LABVIEW interfacing software along with the data acquisition system has been installed to record each measurement.

Two methods have been adopted to perform tests. For both methods, the operating conditions have been set by adjusting the opening of the valve, by regulating the temperature of the preheater and by modifying the water (or glycol) temperature in the test section. In the first method, the main parameter was the test section water (or glycol) temperature and for each test, the mass flow rate was changed. In the second method, the main parameter was the mass flow rate and a new test section water or glycol temperature was set for each test. Besides, a digital camera and Speed Cam were used to visualise the flow pattern at the test section outlet. The camera was put in place at the outlet of the test section. In the other side of the test section there was a source of illumination which was switched on for few seconds only when a video was recorded in a computer kept alongside.

Before performing a test, the system was launched and steady state was reached in about thirty minutes. This procedure was very important for the calibration of the system. Then, the tank of helium was opened, followed by opening of the FC-72 tank, and a value for the water or glycol temperature and for the sub-cooled temperature were chosen. The first test was always performed without FC-72 flow. The test without FC-72 flow was very important in both methods to estimate the heat loss from the thermo-physical system. The

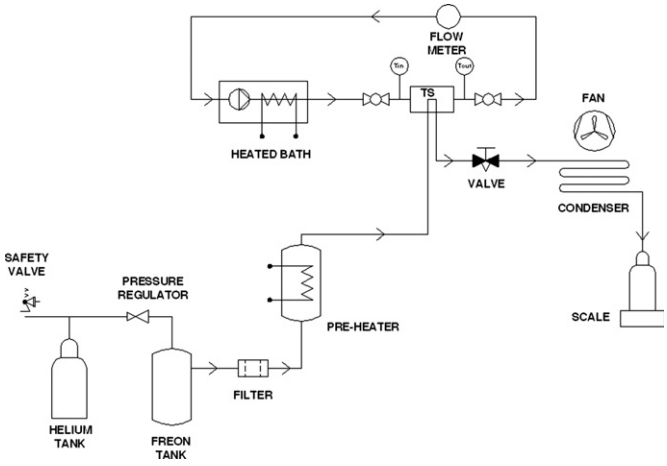

Fig. 1. Schematic of the experimental apparatus.

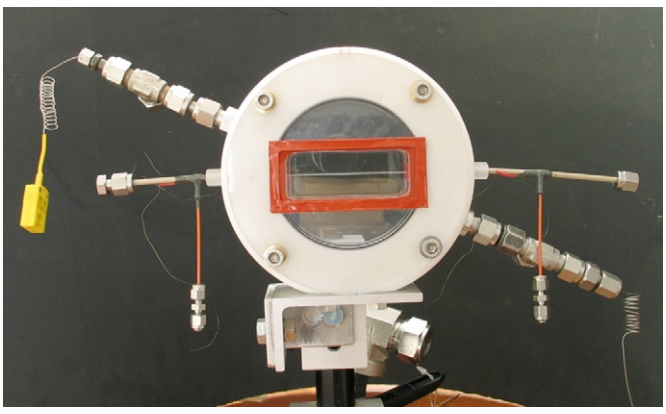

Fig. 2. Test section.

Table 1
Details of the components.

Test section parameter			
Pool		Tube	
Parameter	Value	Parameter	Value
Diameter	81.4 mm	Internal diameter	0.48 mm
Layer	27.3 mm	External diameter	0.8 mm
Length	28 mm	Length	102 mm

evolution of each parameter was monitored by the LABVIEW software. After steady condition is reached, the LABVIEW software and the data acquisition system were launched for one or two minutes.

For tests with FC-72 flow, the valve was opened and value for the FC-72 mass flow rate was chosen. For each experiment, after the opening of the valve, when the mass flow rate was fixed, the procedure was the same as the procedure without FC-72 flow. Couple of minutes was required in order to reach steady condition for all the parameters and then the LABVIEW software was launched. In the case of FC-72 flow tests, Speed Cam software was launched to record the flow pattern at the test section outlet at 2000 fps. Before using the software, two things were noted: firstly the contrast in order to obtain a distinct picture, secondly the number of frames per second. When everything was set, the light was switched on for few seconds and a video was recorded. The light and the Speed Cam software were stopped. The video was watched and only a part of the video for about 200 frames was recorded in the computer.

Following the suggestions of Kline and McClintock [24], the uncertainty has been evaluated for the estimation of heat transfer coefficient and the vapour quality. The uncertainty analysis has been shown in Appendix I and the uncertainty in the heat transfer coefficient and the vapour quality are within ±2.12% and ±0.1086%, respectively.

3. Data reduction

3.1. Parameter calculation

For the FC-72 and the water (or glycol),

$$Q_{FC-72} = \dot{m}_{FC-72} Cp_{FC-72} \Delta T_{FC-72} = \dot{m}_{FC-72} Cp_{FC-72} (T_{FC-72,out} - T_{FC-72,in})$$

$$Q_{wat} = \dot{m}_{wat} Cp_{wat} \Delta T_{wat} = \dot{m}_{wat} Cp_{wat} (T_{wat,out} - T_{wat,in})$$

The heat delivered to FC-72 is determined by an energy balance:

$$Q_{wat} = Q_{FC-72} + Q_{loss}$$

The heat loss is function of the ΔT between the water (or glycol) temperature and the room temperature. In a test where water (or glycol) temperature and room temperature are set, and where there is no FC-72 flow, the following can be written:

$$Q_{wat} = Q_{loss}$$

Now, the heat delivered to the FC-72 is

$$Q_{FC-72} = Q_{wat} - Q_{loss}$$

For each experiment, the heat transfer coefficient is to be determined. In the case of single-phase flow and in the case of two-phase flow, the variable LMTD, ΔT_{LM} is needed for this purpose. LMTD (log-mean temperature difference) is:

■ In single − phase flow :

$$\Delta T_{LM,sp} = \frac{(T_w - T_{FC-72,in}) - (T_w - T_{FC-72,out})}{\ln\left(\frac{T_w - T_{FC-72,in}}{T_w - T_{FC-72,out}}\right)}$$

■ In two − phase flow :

$$\Delta T_{LM,tp} = \frac{(T_w - T_{sat}) - (T_w - T_{FC-72,in})}{\ln\left(\frac{T_w - T_{sat}}{T_w - T_{FC-72,in}}\right)}$$

We have:

$$Q_{FC-72} = \frac{\Delta T}{R} = \frac{T_{w,ext} - T_{w,int}}{R}$$

$$T_{w,int} = T_{w,ext} - R \cdot Q_{FC-72}$$

The expression for R is given by:

$$R = \frac{1}{2\pi \cdot \lambda_{glass} \cdot L} \ln\left(\frac{r_{ext}}{r_{int}}\right)$$

Therefore, we have,

■ In single − phase flow : $h_{sp} = \frac{Q_{FC-72}}{\Delta T_{LM,sp} \cdot S_{int}}$

■ In two − phase flow : $h_{tp} = \frac{Q_{FC-72}}{\Delta T_{LM,tp} \cdot S_{int}}$

The outlet vapour quality is given by

$$x = \frac{h_{out} - h_{sat}}{H_{lv}} = \frac{Cp \cdot (T_{out} - T_{sat})}{H_{lv}}$$

FC-72 properties are given by the polynomial relations (Table 2) in terms of temperature.

The accurate channel heated length required to evaluate the heat transfer coefficient is not known. It can be seen from Fig. 2, the pool and the channel are linked with red connectors. The problem

Table 2
Polynomial relations for calculating FC-72 properties.

Coefficient for the calculation of FC-72 properties								
Name	Expression	Coefficients						
		a	*b*	*c*	*d*	*e*	*f*	*g*
Cp	$1000 \cdot (a + b \cdot T)$	1.0096	1.55×10^{-3}					
μ_l	$a \cdot (T + 273.15)^3 + b \cdot (T + 273.15)^2 c \cdot (T + 273.15) + d$	-5.924×10^{-10}	6.333×10^{-7}	-2.286×10^{-4}	2.821×10^{-2}			
λ	$a \cdot (b \cdot (T + 273.15)^2 + c \cdot (T + 273.15) + d)$	9.0754×10^{-2}	8.9897×10^{-9}	-1.293×10^{-3}	1			
H_{lv}	$1000 \cdot (a + b \ln(P) + c/P + d \cdot P + e \cdot P^2)$	88.3048	−5.239	−0.1398	−3.8508	0.27063		
T_{sat}	$a + b \cdot \ln(P) + c/P + d \cdot P + e \cdot P^2$	324.6304	24.098	0.5967	4.2899	0.2159		
ρ_l	$a \cdot T^6 + b \cdot T^5 + c \cdot T^4 + d \cdot T^3 + e \cdot T^2 + f \cdot T^1 + g$	-1.618×10^{-11}	-1.269×10^{-9}	1.027×10^{-6}	-4.239×10^{-4}	4.973×10^{-2}	−4.014	1.755×10^3

Table 3
Evaluation of heated length.

Evaluation of the heated length from the pixel calculation of pictures							
Test 1		Test 2		Test 3		Test 4	
Min.	Max.	Min.	Max.	Min.	Max.	Min.	Max.
71.8 mm	74.8 mm	70.5 mm	74.4 mm	71 mm	74.5 mm	70.9 mm	74.7 mm

is that it is not known apriori that water (or glycol) could enter into the connectors and in the case of the entrance of water (or glycol), how deep it could go. To find the precise heated length, therefore, two methods have been adopted. The first one is analysing some pictures of the pool and the second one is comparing the heat transfer coefficient with the heat transfer coefficient obtained from the Gnielinski [25] correlation.

Gnielinski [25] correlation is given by:

$$Nu_m = \frac{\xi\cdot(Re-1000)\cdot Pr}{1+12.7\sqrt{\xi}\cdot(Pr^{2/3}-1)}\cdot\left[1+\left(\frac{D_{int}}{L}\right)^{2/3}\right]$$

$$\xi = \frac{(1.82\log(Re)-1.64)^{-2}}{8}$$

$$Nu = Nu_m\cdot\left(\frac{Pr}{Pr_w}\right)^{0.11}$$

A quick evaluation of the heated length from Fig. 2 gives a first approximation. With this method, we have the heated length given in Table 3.

To have an experimental evaluation of the heated length, the difference between the heat transfer coefficient based on the Gnielinski [25] correlation and the single-phase heat transfer coefficient based on the expression above is calculated as shown in Fig. 3.

To determine the heated length, the area where all the graphs are under 5% has been taken into consideration. This area corresponds with a heated length of 73 mm. The comparison between the last result and the results obtained from the pixel calculation is shown in Table 4.

Table 4
Comparison between the experimental data and the (Gnielinski 1976) correlation.

Difference between the two methods							
Test 1		Test 2		Test 3		Test 4	
Min.	Max.	Min.	Max.	Min.	Max.	Min.	Max.
1.64%	2.47%	3.42%	1.92%	2.74%	2.05%	2.88%	2.33%

73 mm as the heated length has been determined for all data reported in this paper.

4. Results and discussion

The creation of the flow pattern map is one of the objectives of the present investigation. To realise this map, several methods have been adopted. For the first method, the water (or glycol) temperature has been kept constant and the inlet FC-72 temperature has also been kept constant; only each test was performed with a new mass flow rate. Thereafter, the mass flow rate and the inlet temperature of the FC-72 were kept constant and the water (or glycol) temperature has been varied. Lastly, the inlet temperature of the FC-72 was varied keeping the other two parameters constant. There was no direct control of the heat flux; it was only indirectly varied.

Data for different heat fluxes have been grouped into low heat flux ($q \leq 50$ kW/m^2), medium heat flux ($50 < q \leq 100$ kW/m^2), high heat flux ($100 < q \leq 150$ kW/m^2) and very high heat flux ($q > 150$ kW/m^2) for presentation and data for different mass fluxes have been grouped into low mass flux ($G \leq 500$ kg/m^2 s), medium mass flux ($500 < G \leq 1500$ kg/m^2 s) and high mass flux ($G > 1500$ kg/m^2 s). The vapour quality was determined at the test section outlet.

Fig. 4 shows all data collated, where, stable flow data and unstable flow data have been plotted as heat flux versus mass flux. From Fig. 4 it is observed that instability and oscillations (back and forth movement of bubbles; but no flow reversal) occurs for mass

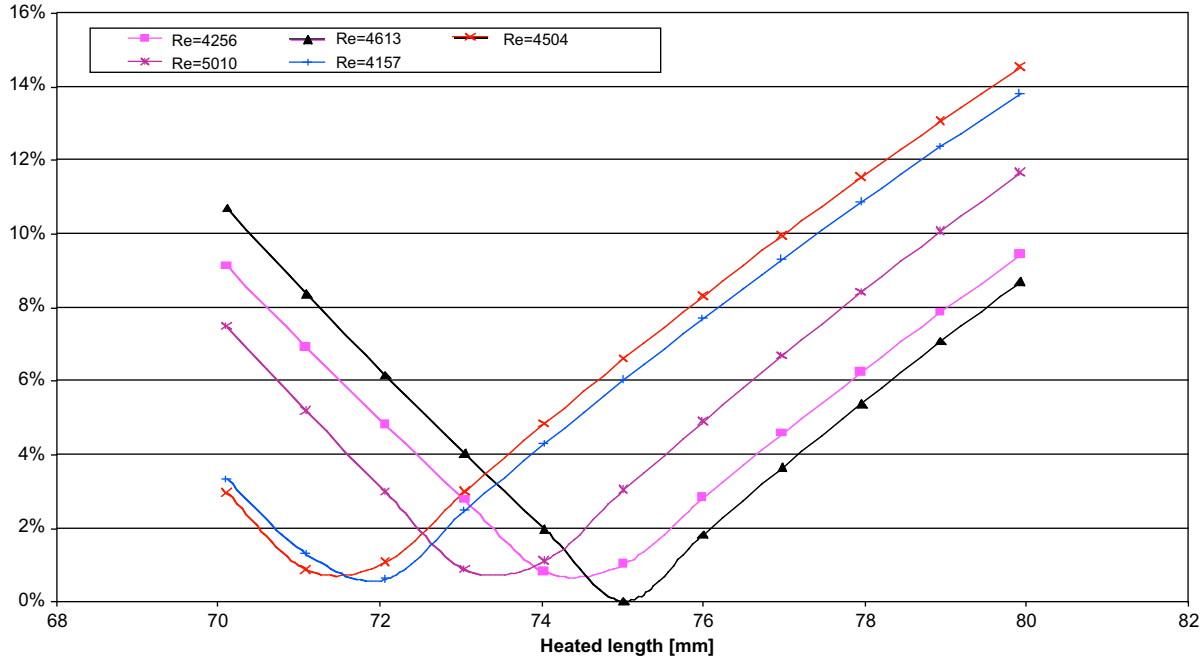

Fig. 3. Difference between experimental and (Gnielinski 1976) heat transfer coefficient as function of the heated length.

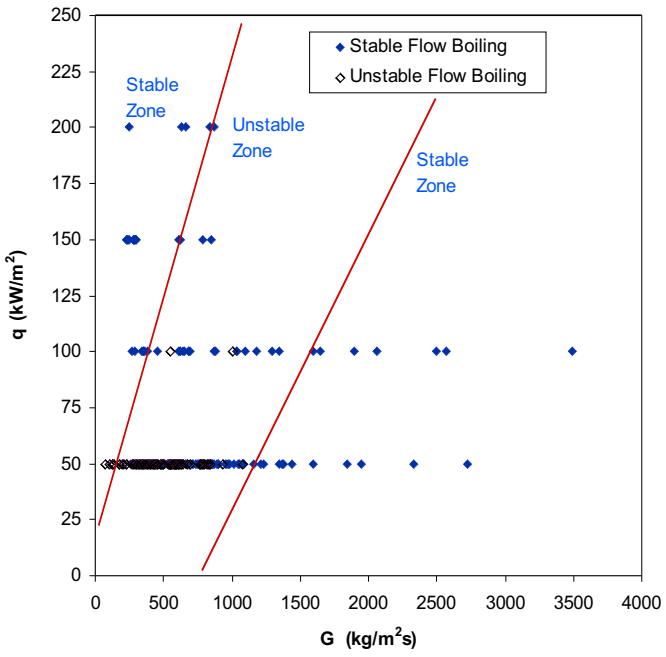

Fig. 4. Stable and unstable flow boiling regimes.

flux less than 1200 kg/m^2 s and heat flux less than 100 kW/m^2; for higher mass flux and heat flux, flow is stable. In Fig. 4, the region in between the two lines may have stable as well as unstable data. The region left of the left line and the region right of the right line have only stable data. Similar flow pattern map in terms of heat flux and mass flux showing the stable and unstable flow boiling regimes in a single microchannel has been observed by Wang et al. [14]. Although Wang et al. [14] have used q/G as a parameter for data analysis, in this work no such parameter could be found and hence no such plotting has been attempted. Wang et al. [14] have also observed stable flow boiling regime with no periodic oscillation and unstable flow boiling regime with short-period oscillation ($<$0.1 s) and long-period oscillation ($>$10 s). Here, in the present investigation, no such classification of oscillation period was observed. Wang et al. [14] observed that the unstable flow boiling regime with long-period oscillation in a single microchannel is smaller than that in parallel microchannels. This implies that flow interaction from neighbouring channels promotes instability in the microchannel. In view of the similarity of the results, this type of flow behaviour is expected with FC-72 flow in parallel microchannels as that have been observed with water flow in microchannels by Wang et al. [14].

Qu and Mudawar [26–28], Steinke and Kandlikar [29,30] and Kandlikar and Balasubramanian [31] have observed reversed flow of vapour in flow boiling phenomenon in parallel minichannels and microchannels. The presence of the parallel channels caused flow reversal giving a path of lower flow resistance. The flow and pressure in the other channels compensated the high pressure due to vapour generation to dissipate through the other channels. Brutin et al. [32] observed a reversed flow and local dry out condition in flow boiling in a single microchannel. No such flow reversal was observed in the present research.

Figs. 5 and 6 show the different flow patterns observed in the present research. No instability was observed during alternating annular/mist flow under high and very high heat flux cases. This flow pattern along with transition instability in a single microchannel is similar to that in single and parallel microchannels as that have been observed by Wang et al. [14]. The trigger mechanism of such instability is venting vapour core due to very rapid expansion. The temporal temperature oscillations of Wang et al. [14] revealed that due to the lack of flow interaction from other channels, the corresponding mass fluxes and oscillation periods of temperature in single microchannel are larger than those in parallel microchannels.

Figs. 7 and 8 show diabatic flow data in terms of heat flux versus exit vapour quality and mass flux versus exit vapour quality. Exit

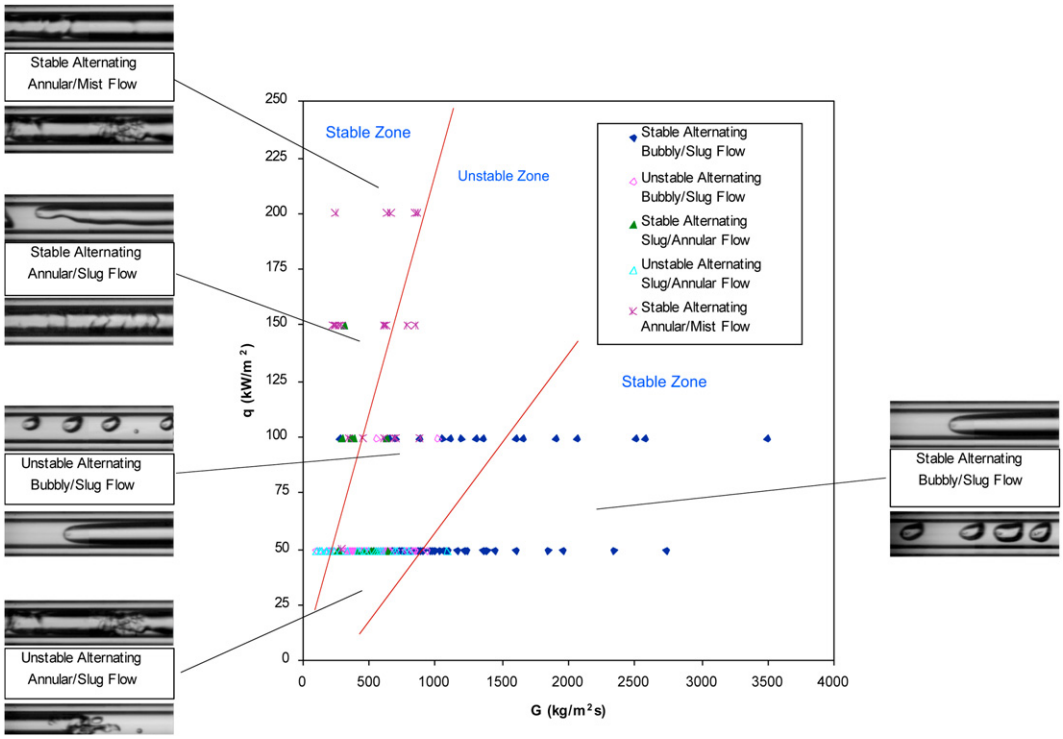

Fig. 5. Different diabatic stable and unstable flow boiling patterns.

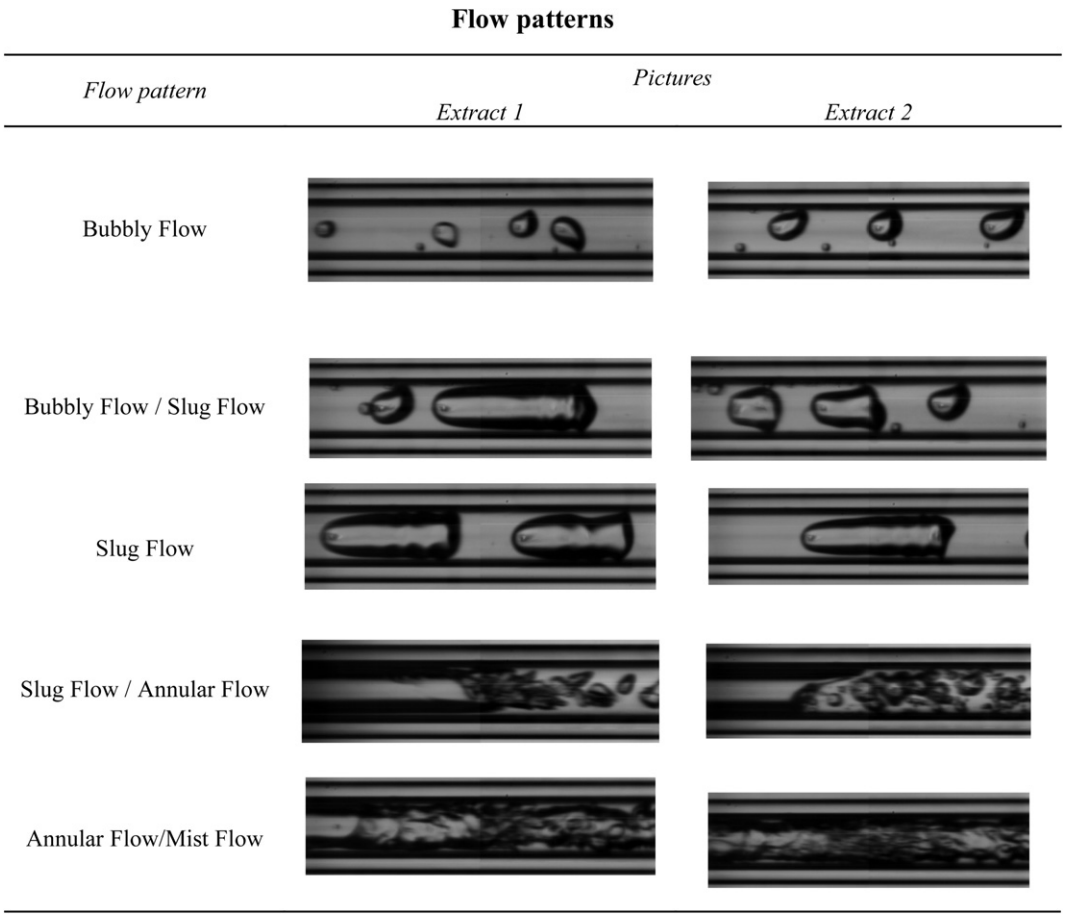

Fig. 6. Different flow patterns.

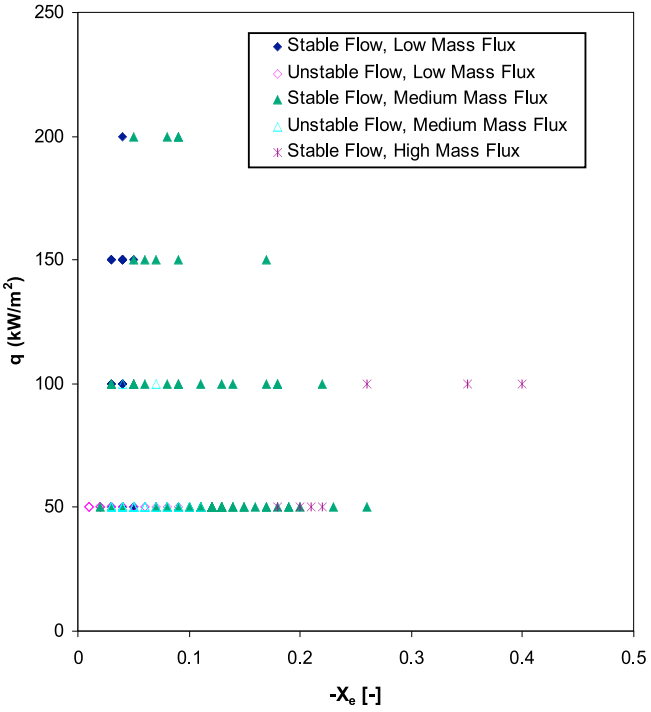

Fig. 7. Heat flux versus exit vapour quality.

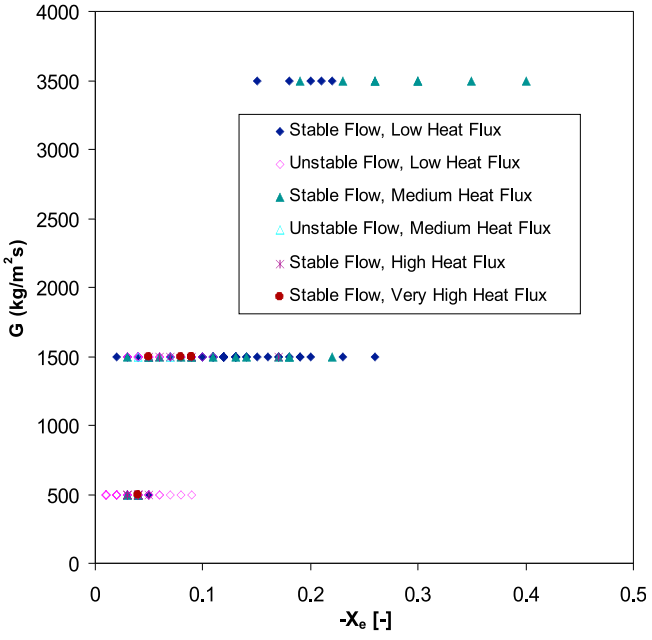

Fig. 8. Mass flux versus exit vapour quality.

vapour quality depends on heat flux, mass flux and inlet FC-72 temperature. As has been observed before, there is alternating stable and unstable bubbly/slug flow, alternating stable and unstable slug/annular flow and stable alternating annular/mist flow. This type of flow pattern has been reported by Wang et al. [33] in parallel microchannels. However, no unsteady flow boiling regime was observed due to the reversed flow of vapour bubbles as has been observed by Wang et al. [33]. In the present research as well as in the work of Wang et al. [33], isolated bubbles were formed near the entrance surface of the microchannel while confined bubbles were observed near the outlet section. Alternating annular/mist flow (Fig. 5) is characterized by an intense mixing of the liquid and the vapour phase. However, sharp wall temperature increase is not expected due to periodic wetting and rewetting process. Near the outlet section, liquid droplets accumulate to rivulets.

Figs. 9 and 10 show the dependence of the flow boiling heat transfer coefficient on the local vapour quality near the outlet section. The range of the measured heat transfer coefficient at the exit from the experiment varied from 0.8 to 27.5 kW/m^2 K, which can be compared with the values of (Wang et al. [33], 9–35 kW/m^2 K), (Hetsroni et al. [34], 10–30 kW/m^2 K), (Chen and Garimella [35], 10–25 kW/m^2 K) and (Qu and Mudawar [27], 20–45 kW/m^2 K).

It is observed from Figs. 9 and 10 that the heat transfer coefficient increased with the increase of vapour quality at higher vapour quality in the present investigation of subcooled boiling region and for the high and very high heat flux and low and medium mass flux. This is perhaps due to a transition from partial to fully developed nucleate boiling. However, at lower vapour quality, the heat transfer coefficient is rather independent of heat flux. This last observation is contradictory to the observation of Wang et al. [33] with saturated boiling.

Kandlikar [36] correlation for flow boiling heat transfer in large diameter conventional tubes has been used in Wang et al. [33], Qu and Mudawar [27], Kandlikar [37] and Kandlikar [1] to correlate microchannel and minichannel heat transfer data. However, although the correlation predicts the general trend of the microchannel flow boiling heat transfer coefficient data, it overpredicts the data at high heat flux and high vapour quality regimes due to the occurrence of local dry out under high heat flux and high vapour quality conditions. In the present work, therefore, this comparison is not done.

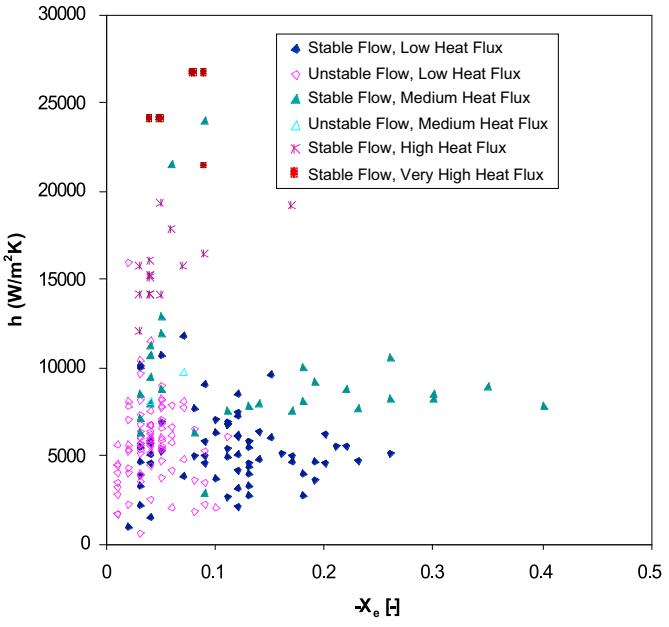

Fig. 9. Heat transfer coefficient versus exit vapour quality, grouped by heat flux.

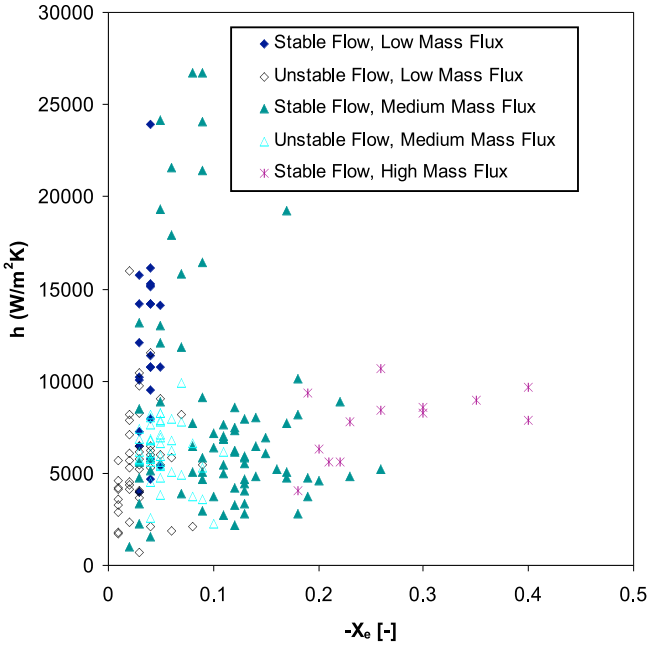

Fig. 10. Heat transfer coefficient versus exit vapour quality, grouped by mass flux.

5. Conclusions

The following conclusions can be drawn from the present work:

1. Heat transfer characteristics of subcooled flow boiling of FC-72 in a single horizontal microchannel are presented.
2. Different flow patterns, both in the stable and unstable flow boiling regimes, have been captured using high speed video camera.
3. Data in small, medium, high and very high heat flux cases under small, medium and high mass flux has been presented.
4. Convective heat transfer coefficients in each flow boiling situation have been calculated and presented.
5. Stable flow boiling with alternating bubbly/slug flow, slug/annular flow and annular/mist flow have been observed for heat flux of 150 kW/m^2 or higher and mass flux of 1500 kg/m^2 s or higher.
6. Back and forth oscillations with flow instabilities have been observed in cases of lower heat and mass fluxes. However, no complete reverse flow in upstream direction has been observed.
7. The heat transfer coefficient increased with the increase of vapour quality at higher vapour quality in the present investigation of subcooled boiling region and for the high and very high heat flux and low and medium mass flux. However, at lower vapour quality, the heat transfer coefficient is rather independent of heat flux.

Acknowledgements

The first author gratefully acknowledges the financial support from the Abdus Salam International Centre for Theoretical Physics, Trieste, Italy and the ENEA Casaccia Research Centre Institute of Thermal Fluid Dynamics, Rome, Italy for the present research.

Appendix I

Uncertainty analysis

All the measured quantities to estimate the heat transfer coefficient and the vapour quality are subject to certain uncertainties because of errors in the measurement. These individual uncertainties as well as the combined effect of these are presented here. The analysis is carried out on the basis of the suggestion made by Kline and McClintock. It is to be noted that the present uncertainty analysis is concerned with the errors pertinent to the measurements made during the investigation. The possible errors in the properties are not included since the physical and transport properties are well documented.

Analysis

Heat transfer coefficient

$$h_{tp} = \frac{Q_{FC-72}}{\Delta T_{LM,tp} \cdot S_{int}}$$

$$\frac{\Delta h_{tp}}{h_{tp}} = \frac{1}{h_{tp}}\left[\left\{\frac{\partial h_{tp}}{\partial Q_{FC-72}}\Delta Q_{FC-72}\right\}^2 + \left\{\frac{\partial h_{tp}}{\partial(\Delta T_{LM,tp})}\Delta(\Delta T_{LM,tp})\right\}^2 + \left\{\frac{\partial h_{tp}}{\partial S_{int}}\Delta S_{int}\right\}^2\right]^{0.5}$$

$$\Rightarrow \frac{\Delta h_{tp}}{h_{tp}} = \left[\left\{\frac{\Delta Q_{FC-72}}{Q_{FC-72}}\right\}^2 + \left\{\frac{\Delta(\Delta T_{LM,tp})}{\Delta T_{LM,tp}}\right\}^2 + \left\{\frac{\Delta S_{int}}{S_{int}}\right\}^2\right]^{0.5}$$

where, following as above,

$$\frac{\Delta Q_{FC-72}}{Q_{FC-72}} = \left[\left(\frac{\Delta \dot{m}}{\dot{m}}\right)^2 + \left(\frac{\Delta T_{FC-72,out}}{T_{FC-72,out} - T_{FC-72,in}}\right)^2 + \left(\frac{\Delta T_{FC-72,in}}{T_{FC-72,out} - T_{FC-72,in}}\right)^2\right]^{0.5}$$

$$\frac{\Delta(\Delta T_{LM,tp})}{\Delta T_{LM,tp}} = \left[\left(\frac{\Delta T_{FC-72,in}}{T_{FC-72,in} - T_{sat}}\right)^2 + \left(\frac{\Delta T_{sat}}{T_{FC-72,in} - T_{sat}}\right)^2 + \left(\frac{\Delta A}{A}\right)^2\right]^{0.5}$$

where

$$A = \ln B \quad \text{with} \quad B = \frac{T_w - T_{sat}}{T_w - T_{FC-72,in}}$$

$$\frac{\Delta A}{A} = \left[\frac{1}{(\ln B)^2}\left\{\frac{\Delta(T_w - T_{sat})}{T_w - T_{sat}}\right\}^2 + \frac{1}{(\ln B)^2}\left\{\frac{\Delta(T_w - T_{FC-72,in})}{T_w - T_{FC-72,in}}\right\}^2\right]^{0.5}$$

$$\frac{\Delta(T_w - T_{sat})}{T_w - T_{sat}} = \left\{\left(\frac{\Delta T_w}{T_w - T_{sat}}\right)^2 + \left(\frac{\Delta T_{sat}}{T_w - T_{sat}}\right)^2\right\}^{0.5}$$

$$\frac{\Delta(T_w - T_{FC-72,in})}{T_w - T_{FC-72,in}} = \left\{\left(\frac{\Delta T_w}{T_w - T_{FC-72,in}}\right)^2 + \left(\frac{\Delta T_{FC-72,in}}{T_w - T_{FC-72,in}}\right)^2\right\}^{0.5}$$

$$\frac{\Delta S_{int}}{S_{int}} = \left\{\left(\frac{\Delta D}{D}\right)^2 + \left(\frac{\Delta L}{L}\right)^2\right\}^{0.5}$$

Vapour quality

$$\frac{\Delta x}{x} = \left\{\left(\frac{\Delta T_{FC-72,out}}{T_{FC-72,out} - T_{sat}}\right)^2 + \left(\frac{\Delta T_{sat}}{T_{FC-72,out} - T_{sat}}\right)^2\right\}^{0.5}$$

The accuracies (Δ) of the measured quantities are as follows:

Temperature from thermocouple: 1 μV giving 0.025 °C
FC-72 mass flow rate: 1 mg/s Water and glycol mass flow rate: 1 g/s
Diameter of microchannel: 1 μm Length of microchannel: 0.1 mm.

References

[1] S.G. Kandlikar, Fundamental issues related to flow boiling in mini channels and micro channels. Exp. Thermal Fluid Sci. 26 (2002) 389–407.
[2] S.G. Kandlikar, Two phase flow patterns, pressure drop and heat transfer during boiling in minichannel flow passages of compact evaporators. Heat Transfer Eng. 23 (1) (2002) 5–23.
[3] J.R. Thome, Boiling in microchannels: a review of experiment and theory. Int. J. Heat Fluid Flow 25 (2004) 128–139.
[4] L.P. Yarin, A. Mosyak, G. Hetsroni, Boiling in microchannels, in: Fluid Flow, Heat Transfer and Boiling in Microchannels. Springer, Berlin, 2009.
[5] S.S. Bertsch, E.A. Groll, S.V. Garimella, Refrigerant flow boiling heat transfer in parallel microchannels as a function of local vapor quality. Int. J. Heat Mass Transfer 51 (2008) 4775–4787.
[6] S.S. Bertsch, E.A. Groll, S.V. Garimella, Review and comparative analysis of studies on saturated flow boiling in small channels. Nanoscale Microscale Thermophys. Eng. 12 (2008) 187–227.
[7] S.S. Bertsch, E.A. Groll, S.V. Garimella, Effects of heat flux, mass flux, vapor quality and saturation temperature on flow boiling heat transfer in microchannels. Int. J. Multiphase Flow 35 (2009) 142–154.
[8] S.S. Bertsch, E.A. Groll, S.V. Garimella, A composite heat transfer correlation for saturated flow boiling in small channels. Int. J. Heat Mass Transfer 52 (2009) 2110–2118.
[9] J.A. Boure, A.E. Bergles, L.S. Tong, Review of two phase flow instability. Nucl. Eng. Des. 25 (1973) 165–192.
[10] L. Tadrist, Review on two phase flow instabilities in narrow spaces. Int. J. Heat Fluid Flow 28 (2007) 54–62.
[11] G. Ribatski, L. Wojtan, J.R. Thome, An analysis of experimental data and prediction methods for two phase frictional pressure drop and flow boiling heat transfer in micro-scale channels. Exp. Thermal Fluid Sci. 31 (2006) 1–19.
[12] S. Kakac, B. Bon, A review of two-phase flow dynamic instabilities in tube boiling systems. Int. J. Heat Mass Transfer 51 (2008) 399–433.
[13] S.V. Garimella, C.B. Sobhan, Transport in microchannels – a critical review. Ann. Rev. Heat Transfer 13 (2003) 1–50.
[14] G.D. Wang, P. Cheng, H.Y. Wu, Unstable and stable flow boiling in parallel microchannels and in a single microchannel. Int. J. Heat Mass Transfer 50 (2007) 4297–4310.
[15] T. Fukano, L. Kariyasaki, Characteristic of gas liquid two phase flow in a capillary tube. Nucl. Eng. Des. 141 (1993) 58–68.
[16] K. Triplett, S. Ghiaasiaan, S. Abdel Khalik, A. LeMouel, B. McCord, Gas liquid two phase flow in microchannels, part I: two phase flow patterns. Int. J. Multiphase Flow 25 (1999) 377–394.
[17] X.F. Peng, H.Y. Hu, B.X. Wang, Boiling nucleation during liquid flow in microchannels. Int. J. Heat Mass Transfer 41 (1998) 101–106.
[18] J.R. Thome, V. Dupont, A.M. Jacobi, Heat transfer model for evaporation in microchannels, part I: presentation of the model. Int. J. Heat Mass Transfer 47 (2004) 3375–3385.
[19] J.R. Thome, V. Dupont, A.M. Jacobi, Heat transfer model for evaporation in microchannels, part II: comparison with database. Int. J. Heat Mass Transfer 47 (2004) 3387–3401.
[20] J.E. Kennedy, G.M. Roach, M.E. Dowling, S.I. Abdel-Khalik, S.M. Ghiaasiaan, S.M. Jeter, Z.H. Qureshi, The onset of flow instability in uniformly heated horizontal microchannels. ASME J. Heat Transfer 122 (2000) 118–125.
[21] G. Hetsroni, A. Mosyak, Z. Segal, E. Pogrebnyak, Two-phase flow pattern in parallel microchannels. Int. J. Multiphase Flow 29 (2003) 341–360.
[22] G. Hetsroni, M. Gurevich, A. Mosyak, R. Rozenbilt, Surface temperature measurement of a heated capillary tube by means of an infrared technique. Meas. Sci. Technol. 14 (2003) 807–814.
[23] G. Hetsroni, D. Klein, A. Mosyak, A. Segal, E. Pogrebnyak, 2003, Convective boiling in parallel microchannels, in: Proc. 1st Int. Conf. Microchannels and

Minichannels, April 24–25, Rochester, N.Y., USA, pp. 59–67, also in Microscale Thermophysical Engineering, vol. 8, pp. 403–421.
[24] S.J. Kline, F.A. McClintock, Describing uncertainties in single-sample experiments. Mech. Eng. 75 (1) (1953) 3–8.
[25] V. Gnielinski, New equations for heat transfer in turbulent pipe and channel flow. Int. Chem. Eng. 16 (1976) 359–368.
[26] W. Qu, I. Mudawar, Measurement and prediction of pressure drop in two phase microchannel heat sinks. Int. J. Heat Mass Transfer 46 (2003a) 2737–2753.
[27] W. Qu, I. Mudawar, Flow boiling heat transfer in two phase micro channel heat sink, I: experimental investigation and assessment of correlation methods. Int. J. Heat Mass Transfer 46 (2003b) 2755–2771.
[28] W. Qu, I. Mudawar, Flow boiling heat transfer in two phase micro channel heat sink, II: annular two phase flow model. Int. J. Heat Mass Transfer 46 (2003c) 2773–2784.
[29] M.E. Steinke, S.G. Kandlikar, Control and effect of dissolved air in water during flow boiling in microchannels. Int. J. Heat Mass Transfer 47 (2004a) 1925–1935.
[30] M.E. Steinke, S.G. Kandlikar, An experimental investigation of flow boiling characteristics of water in microchannels. ASME J. Heat Transfer 126 (2004b) 518–526.
[31] S.G. Kandlikar, P. Balasubramanian, An experimental study on the effect of gravitational orientation on flow boiling of water in 1054 × 197 μm parallel minichannels. ASME J. Heat Transfer 127 (8) (2005) 820–829.
[32] D. Brutin, F. Topin, L. Tadrist, Experimental study of unsteady convective boiling in heated minichannels. Int. J. Heat Mass Transfer 46 (2003) 2957–2965.
[33] G.D. Wang, P. Cheng, A.E. Bergles, Effects of inlet outlet configurations on flow boiling instability in parallel microchannels. Int. J. Heat Mass Transfer 51 (2008) 2267–2281.
[34] G. Hetsroni, A. Mosyak, E. Pogrebnyak, Z. Segal, Explosive boiling of water in parallel microchannels. Int. J. Multiphase Flow 31 (2005) 371–392.
[35] T. Chen, S. Garimella, Measurements and high speed visualizations of flow boiling of a dielectric fluid in a silicon microchannel heat sink. Int. J. Multiphase Flow 32 (2006) 957–971.
[36] S.G. Kandlikar, A general correlation for saturated two phase boiling heat transfer inside horizontal and vertical tubes. ASME J. Heat Transfer 112 (1990) 219–228.
[37] S.G. Kandlikar, Heat transfer mechanisms during flow boiling in microchannels. ASME J. Heat Transfer 126 (2004) 8–16.